Composites: Part B 52 (2013) 172–181

Contents lists available at SciVerse ScienceDirect

Composites: Part B

journal homepage: www.elsevier.com/locate/compositesb

Can flax replace E-glass in structural composites? A small wind turbine blade case study

Darshil U. Shah, Peter J. Schubel *, Mike J. Clifford

Polymer Composites Group, Division of Materials, Mechanics and Structures, Faculty of Engineering, The University of Nottingham, Nottingham NG7 2RD, UK

ARTICLE INFO

Article history:
Received 26 October 2012
Received in revised form 27 March 2013
Accepted 7 April 2013
Available online 18 April 2013

Keywords:
A. Polymer–matrix composites (PMCs)
B. Elasticity
B. Strength
D. Mechanical testing
Natural fibres

ABSTRACT

In directly addressing the question, 'can flax replace E-glass as a reinforcement for structural composites?', this manuscript adopts a novel comparative case study approach to investigate the manufacture and mechanical testing of full-scale 3.5-m composite rotor blades (suitable for 11 kW turbines) built from flax/polyester and E-glass/polyester.

The resin transfer moulded flax blade is 10% lighter (fibre mass saving of 45%) than the identical construction E-glass blade. Static flap-bending tests, conducted in accordance to certification standards, confirm that like the E-glass blade, the flax blade satisfies the structural integrity requirements under 'normal operation' and 'worst case' loading. It is consequently claimed that flax is a potential structural replacement to E-glass for similar composite small wind turbine blade applications.

The failure root bending moment and corresponding tip displacement of the flax blade are 11.6 kN m and 2300 mm, respectively. The blades exhibit distinctly different load–deflection curves and failure modes. The mean flexural rigidity of the flax and E-glass blades are estimated to be 24.6 kN m^2 and 43.4 kN m^2, respectively. It is interesting to find that although flax fibres and their composites are generally recognized for their stiffness, a flax blade cannot compete against an E-glass blade in terms of stiffness.

1. Introduction

Plant fibres offer several economical, technical and ecological advantages over synthetic fibres in reinforcing polymer composites (Table 1) [1,2]. Due to the relative abundance, low cost of raw material, low density, high specific properties, and positive environmental profile of plant fibres like flax, hemp and jute, they have been marketed as prospective substitutes to traditional composite reinforcements, specifically E-glass [1–3]. As 87% of the 8.7 million tonne global fibre reinforced plastic (FRP) market is based on E-glass composites (GFRPs) [4], plant fibres and their composites have a great opportunity for development and market capture.

Although the use of plant fibres (non-wood and non-cotton) in reinforced plastics has tripled to 45,000 tonnes over the last decade [5–7], plant fibre composites (PFRPs) make up only ~1.9% of the 2.4 million tonne EU FRP market (Fig. 1) [6]. Notably, the use of carbon fibre composites is lower than the use of biocomposites and on the same level as the use of PFRPs (Fig. 1) [4,6]. It is of interest to note that while PFRPs were developed and are viewed as alternatives to GFRPs [2,8], they have mainly replaced wood fibre reinforced thermosets in the EU automotive industry [9,10]. By commercial application, over 95% of PFRPs are being used for non-structural automotive interior components (such as door and instrumental panels) [6,7,11–13]. Other than automotive applications, PFRPs are being considered for applications in (i) construction and infrastructure (such as beams, roof panels, bridges) [7,12,14–21], (ii) sports and leisure (for boat hulls, canoes, bicycle frames, tennis rackets) [7,9,12,15,20,21], (iii) furniture and consumer goods (such as packaging, cases, urns, chairs, tables, helmets, ironing boards) [6,7,9,12,15,16,18–21], and (iv) pipes and tanks (for water drainage and transportation) [7,12,14,19,21–23]. In many of these applications, plant fibres are being employed primarily as light, cheap and 'green' reinforcements, playing little or no structural role.

Interestingly, this is different to what was envisaged 70 years ago, when the potential of plant fibres as structural reinforcing agents was acknowledged by pioneers like Ford to manufacture the first 'green car' with an all-plastic-body using 70 wt.% lignocellulosic fibres in a soybean oil based phenolic matrix [24,25]. Ford was even able to demonstrate the impact resistance of the material by famously taking a sledgehammer onto the car's deck lid [24]. At the same time, Aero Research Ltd., developed Gordon Aerolite, a flax/phenolic composite, to replace aluminium sheets for building

* Corresponding author. Tel.: +44 (0)1159513979.
E-mail address: peter.schubel@nottingham.ac.uk (P.J. Schubel).

1359-8368 © 2013 The Authors. Published by Elsevier Ltd. Open access under CC BY license.
http://dx.doi.org/10.1016/j.compositesb.2013.04.027

Table 1
Comparison between plant fibers and E-glass [1].

	Properties	Plant fibres	E-Glass fibre
Economy	Annual global production (tonnes)	31,000,000	4,000,000
	Distribution for FRPs in EU (tonnes)	Moderate (40,000)	High (600,000)
	Cost of raw fibre (£/kg)	Low (~0.5–1.5)	Low (1.3)
Technical	Density (g cm^{-3})	Low (~1.35–1.55)	High (2.66)
	Tensile stiffness (GPa)	Moderate (~30–80)	Moderate (73)
	Tensile strength (GPa)	Low (~0.4–1.5)	Moderate (2.0–3.5)
	Tensile failure strain (%)	Low (~1.4–3.2)	Low (2.5)
	Specific tensile stiffness (GPa/g cm^{-3})	Moderate (~20–60)	Low (27)
	Specific tensile strength (GPa/g cm^{-3})	Moderate (~0.3–1.1)	Moderate (0.7–1.3)
	Abrasive to machines	No	Yes
Ecological	Energy consumption (MJ/kg of fibre)	Low (4–15)	Moderate (30–50)
	Renewable source	Yes	No
	Recyclable	Yes	Partly
	Biodegradable	Yes	No
	Toxic (upon inhalation)	No	Yes

the structural members of Spitfire fuselages for British military aircrafts during the Second Great War [26].

Despite the current growing interest in PFRPs for (semi-)structural applications and glimpses of their impressive mechanical performance, to date, there are only limited scientific studies that conclusively show the suitability of PFRPs over GFRPs for load-bearing applications.

1.1. Reinforcements for rotor blades: plant fibres or E-glass?

The Wind Energy Materials Group (within the Polymer Composites Research Group) at The University of Nottingham has been involved with the design and manufacture of composite wind turbine blades. Recently, the Group has been investigating the potential of sustainable plant fibre reinforcements as a replacement to conventional E-glass reinforcements in small wind turbine (SWT) blades. This investigation has large implications owing to the unprecedented growth of the global SWT industry [27]. It is estimated that by 2020, the total UK small wind turbine capacity will exceed 1300 MW, through the installation of more than ~400,000 SWTs [27]. Assuming these are 3-bladed systems, more than 1 million composite blades will need to be manufactured [27].

The blades of a wind turbine are a critical and costly component of a wind turbine system. Having a service life of 20–30 years and cycling in excess of 150 rpm, small rotor blades ($\Phi < 16$ m, suitable for <100 kW turbines) are designed against several major structural conditions including strength, stiffness and tip deflection during operational loading (design wind speeds of 11.9 m s^{-1}) and severe loading (extreme wind speeds of 59.5 m s^{-1}), as well as very high numbers of fatigue cycles (>10^9 cycles) during service. Naturally, for certification of the SWT blades, the structural integrity of the blade needs to be demonstrated by analysis and full-scale mechanical tests, as per BS-EN 61400-2:2006 [28] and BS-EN 61400-23:2002 [29].

Recently, the authors of this article have shown that a PFRP SWT blade can survive the design fatigue loads for the required 20-year life [30,31]. This manuscript details a novel comparative case study on the manufacture and mechanical testing of 3.5 m composite rotor blades, suitable for an 11 kW SWT, built from flax/polyester and E-glass/polyester. Firstly, this article compares the weight, cost and manufacturing properties of the two blades. Secondly, through static mechanical testing of the blades, in accordance to the certification standards [28,29], their mechanical properties are compared.

2. Design and manufacture of blades

2.1. Blade design summary

The study blade is 3.50 m in length, with an average chord length of 0.29 m. For improved blade efficiency, an aerodynamically optimised blade shape, generated through an in-house developed design software (*BladeShaper v2.0*) considering (i) blade element momentum theory including wake rotation, (ii) turbine performance, and (iii) part manufacturability, was employed.

To achieve the desired structural performance, based on past experience, a conventional blade construction is used (Fig. 2). The blade consists of a CNC machined core and fibre reinforced composite structural blister caps and constant-thickness outer shell. The core provides resistance against buckling, the unidirectional fibre reinforced blister caps provide maximum axial (tensile) and bending (flexural) stiffness and strength, and the multiaxial fibre reinforced outer skin provides resistance against torsion-related shear loads. The composite material has a nominal fibre

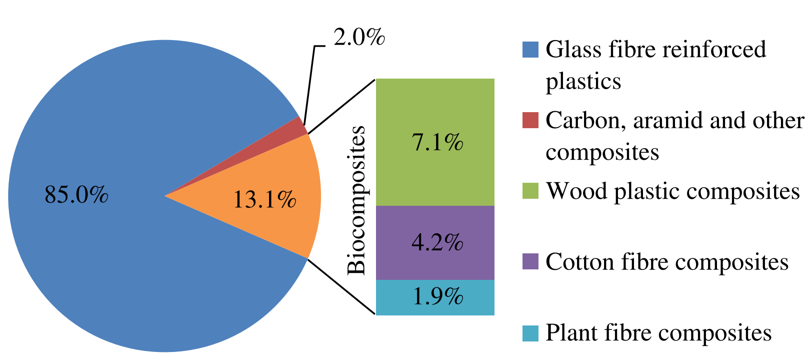

Fig. 1. PFRPs accounted for ~1.9% of the 2.4 million tonne EU FRP market in 2010 [6].

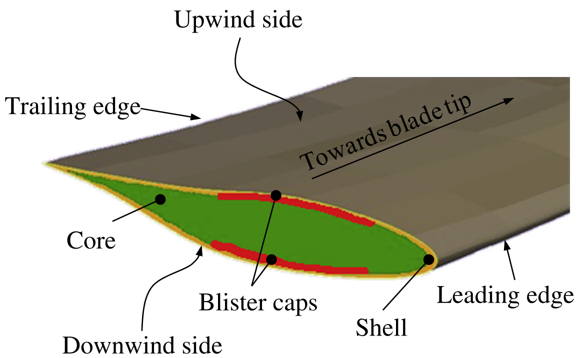

Fig. 2. Construction of the composite blade.

volume fraction of 32–38%. The ratio of multiaxial reinforcement (in the shell) to unidirectional reinforcement (in the blister caps) is ~180–250 wt.%.

2.2. Blade manufacture

Two identical blades were manufactured using flax and E-glass as reinforcements, employing the same stacking sequence. Low-twist (20 tpm, 400 tex) wet-spun flax rovings were sourced from Safilin (France). Prior to spinning, the dew-retted flax slivers were soaked in a hot dilute solution of caustic soda. This process not only improves roving regularity, but would also promote better fibre/matrix adhesion and thus composite mechanical properties by removing surface impurities (wax, oil, pectin, lignin), revealing individual fibrils ('defibrillation') and generating a rough surface topography [32]. Formax (UK) Ltd., produced stitched aligned fabrics (unidirectional [0] and balanced multiaxials ([±45], [0,±45])) with these flax rovings. Stitched aligned fabrics of E-glass were also sourced from Formax (UK) Ltd. The E-glass fibres were surface treated with an epoxy size, that is suited to both polyester and epoxy resin systems. For blade manufacture, the reinforcements were employed as-received, without any preconditioning.

The tensile and fatigue properties of polyester composites made from these reinforcements have been previously examined in [33,34]; some of the characterised properties are presented in Table 2. It is observed that while unidirectional E-glass composites have significantly better mechanical properties than unidirectional flax composites, the specific tensile stiffness of the composites and the effective tensile stiffness of the fibres are comparable.

The blades were manufactured using an unsaturated polyester resin in a light resin transfer moulding (LRTM) process. Both blades took ~1.5 h to infuse showing that using plant fibre reinforcements does not significantly alter infusion times. Post cure was conducted at 40 °C for 2 h. The manufactured flax/polyester and E-glass/polyester blades are shown in Fig. 3. A manufacturing advantage of using flax over E-glass is that the former do not cause itching during handling and are non-hazardous if inhaled.

Note that as the flax reinforcements were in the form of rovings (rather than twisted yarns), they were loose (rather than compact). The bulkiness of the fabric layers implied that closing the tool after placing the fabric was difficult, particularly at the maximum chord length where there is also a large variation in cross-sectional thickness. Nonetheless, as increasing yarn twist has several detrimental effects on PFRP performance including lowered permeability, hindered impregnation, formation of impregnation related voids and significant loss in orientation efficiency; rovings are preferred for PFRP components [35].

2.3. Comparison of mass properties

Fig. 4a shows the difference in mass of the flax and E-glass blades. Weighing at 23.3 ± 0.1 kg, the flax blade is 10% lighter than the E-glass blade (25.8 ± 0.1 kg). Interestingly, the density of the flax reinforcement was measured to be 1.57 g cm^{-3}, which is 60% that of E-glass (2.66 g cm^{-3}) [33]. The reason why the flax blade is only 10% lighter than the E-glass blade is that the fibre accounts for only 18% and 30% of the flax and E-glass blade masses. Directly comparing the fibre masses allows to appreciate the weight savings that flax provides; while the E-glass blade has 7.7 kg of fibre, the flax blade has only 4.2 kg of fibre. That is, using flax, rather than E-glass, reduces the fibre mass by 45%.

As Fig. 4a illustrates, the mass of the core is identical in both blades and accounts for 32–36% of the blade mass. Interestingly, the resin accounts for 38% of the E-glass blade mass but 46% of the flax blade mass. The intake of 1 kg more resin in the flax blade is possibly due to (i) the slightly lower volume of fibre (accounting for ~0.3 kg of extra resin), and (ii) a cavity forming over certain regions of the blade (specifically, at the maximum chord length) resulting from the deflection of the mould tool.

Note that the volume of fibre reinforcement used in both blades is similar at 0.0027–0.0029 m^3. The fibre volume fraction in the composite part of the blades is calculated to be 23–26% (Table 3). The lower fibre weight fraction of the flax composite, compared to the E-glass composite (Table 3), is solely due to the difference in densities of the flax and E-glass fibres. Therefore, the difference in fibre weight fraction cannot be avoided (if the composites have the same fibre volume fraction).

Table 2
Tensile and fatigue properties of unidirectional flax/polyester and E-glass/polyester composites (from [33,34]).

	Property		Flax	E-glass	Flax/E-glass
Physical	Fibre volume fraction	%	30.9	42.8	
	Density	g cm^{-3}	1.31	1.79	0.732
Tensile	Composite stiffness	GPa	23.4	36.9	0.634
	Composite specific stiffness	GPa/g cm^{-3}	17.9	20.6	0.869
	Effective fibre stiffness[a]	GPa	67.6	81.6	0.828
	Composite strength	MPa	277	826	0.335
	Composite specific strength	MPa/g cm^{-3}	213	461	0.462
	Effective fibre strength[a]	MPa	883	1920	0.460
	Composite failure strain	%	1.70	1.90	0.895
Physical	Fibre volume fraction	%	26.9	30.0	0.897
	Density	g cm^{-3}	1.29	1.64	0.787
Fatigue ($R = 0.1$)	Single cycle strength	MPa	236	567	0.416
	Fatigue strength at 10^6 cycles	MPa	115	204	0.564

[a] The effective fibre properties are 'back-calculated' using the rule of mixtures.

Fig. 3. Images of the (a) flax/polyester and (b) E-glass/polyester blades.

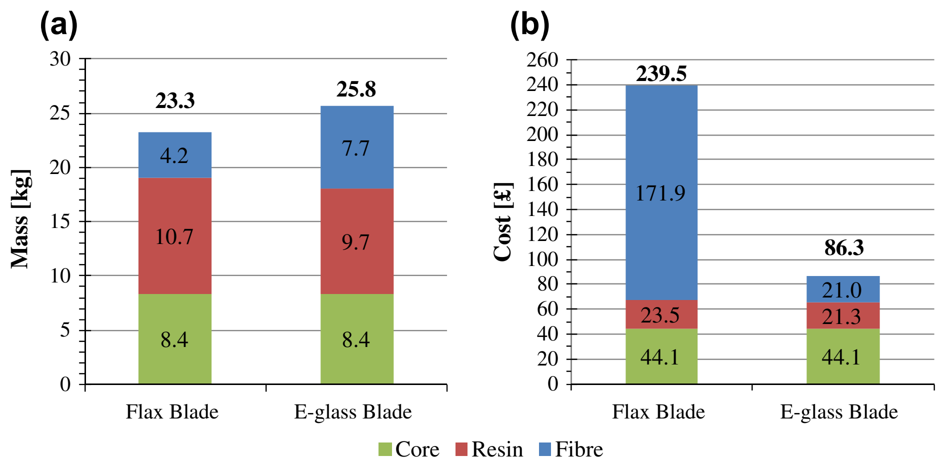

Fig. 4. Comparison of the (a) mass and (b) materials cost of the flax and E-glass blades.

Table 3
Calculated overall fibre weight and volume fractions in the composite part of the blades (excluding the core).

	Flax blade	E-glass blade
Density (g cm^{-3})	1.28	1.59
Fibre weight fraction (%)	28.2	44.3
Fibre volume fraction (%)	22.9	26.4

The centre of gravity C_g from the blade root is 1.26 ± 0.01 m for the flax blade and 1.29 ± 0.01 m for the E-glass blade. The C_g is fairly similar for both blades, as the blade construction and fabric stacking sequence is identical.

2.4. Comparison of materials cost

Fig. 4b presents the difference in material cost of making the flax and E-glass blades. The materials cost for the flax blade amounts to ~£240, making it approximately three times more expensive than the E-glass blade. The material cost of the core (at 5.28 £/kg) and the polyester resin (at 2.20 £/kg) are almost identical for the two blades, amounting to ~£65. Fig. 4 shows that despite requiring less fibre in a flax blade, the fibre cost of the flax blade is 8 times that of the E-glass blade.

Unlike E-glass, costs of flax reinforcements increase tremendously with processing steps. This is because (i) E-glass reinforcements are an established mature market, and (ii) the processing (and incurred costs) of flax and E-glass reinforcements is different. As Table 4 highlights, under current market conditions, aligned flax reinforcements are more expensive than aligned E-glass reinforcements at every stage: raw fibre, yarn/roving and aligned fabric. Raw flax itself is barely cost-competitive against raw E-glass [17,36]. Interestingly, the cost of non-woven mats of flax fibres is comparable to (or even lower than) that of E-glass (Table 4). This is possibly a result of the fact that naturally discontinuous plant fibres are readily (without much processing) useable in the production of non-wovens. It is thus not surprising that current industrial applications of PFRPs are principally based on non-woven precursors [6]. However, to make aligned fabric reinforcements, staple plant fibres like flax need to be first processed into yarns/rovings, unlike E-glass which is a synthetic filament. Flax rovings/yarns are up to 10 times more expensive than E-glass. Madsen [37] have also commented on the high market price of such plant fibre yarns. In addition, the actual cost associated with aligned fabric manufacture needs to be accounted. The flax reinforcements were specially produced for this study; the costs for the multi-axial fabrics (300–600 gsm) ranged from 13.8 £/m^2 to 22.0 £/m^2. E-glass fabrics (300–600 gsm) were off-the-shelf items, which typically cost 1.80 £/m^2. By weight, the cost of aligned flax fabric is 6–15 times greater than that of aligned E-glass fabric. In essence, the development of

Table 4
Flax is costlier than E-glass at every stage. Costs for raw fibre, yarn/roving and aligned fabrics are obtained from materials suppliers (and assumed indicative of the market prices) as of December 2012. Costs for non-woven mats are from [37].

Cost of reinforcement	Flax[a]	E-glass	Flax/E-glass
Raw fibre (£/kg)	1.5	1.3	1.2
Yarn/roving (£/kg)	10.0–13.0	1.3	7.7–10.0
Aligned fabric (£/kg)	36.7–45.9	3.0–6.0	6.1–15.3
Non-woven mat (£/kg)	1.5	2.2	0.7

[a] Note that the prices of the flax reinforcements quoted here are based on small quantities and should only be used as guidelines. Prices reduce significantly with higher quantities (>5 tonnes), but also depend on other factors such as market conditions and fibre quality.

low-cost aligned plant fibre semi-products is a critical and potentially limiting factor in encouraging the future industrial use of PFRPs, as an alternative to GFRPs.

3. Mechanical testing of blades

Upon the design and manufacture of the two blades, their structural integrity was assessed through design load analysis and full-scale mechanical tests, as per BS-EN 61400-2:2006 [28] and BS-EN 61400-23:2002 [29]. This section details the flap-wise static testing of the two blades.

3.1. Description and derivation of test loads

3.1.1. Design loads

The SWT, for which the blades are to be used, is an 11 kW Class-II horizontal axis 3-bladed upwind stall regulated turbine, with a rigid hub, cantilever blades, active yaw mechanism and fixed pitch. Hence, design loads for the blades can be determined using simplified conservative load equations in [28]. For the flap-wise static testing of the blade, as per [29] it is the blade root bending moment M_{yB} (acting to bend the blade tip downwind) that is of interest. [29] acknowledges that stresses caused by radial loads (F_{zB}) are relatively low. This is confirmed through a simple stress analysis at the blade root. At the design wind speed (11.9 m s^{-1}) and design rotor speed (170 rpm) under normal operating conditions (*Load Case A* in [28]), the flax and E-glass blade experience a radial load of 23.6 kN and 26.2 kN, respectively (due to difference in masses). The resultant mean stress at the blade root is only 1.22–1.35 MPa.

Typically, the blade is tested against the calculated blade root bending moment M_{yB} under normal operating conditions (*Load Case A* in [28]) and worst case loading. Note that this turbine has an active yaw mechanism which ensures that when subjected to extreme gusts (*Load Case H* in [28] at extreme wind speed of 59.5 m s^{-1}), the turbine is parked at 90° yaw angle, leading to minimal exposure. Using known values for constants, blade/turbine parameters and wind condition parameters, the design loads on the blade have been determined for the several load cases [38]. For this particular turbine setup, the worst case loading was found to occur when there is a yaw error of 30° (*Load Case C* in [28] at design wind speed of 11.9 m s^{-1}). Conveniently, blade root bending moment M_{yB} at *Load Case A* and *Load Case C* are not a function of blade mass, and hence are the same for both the blades.

3.1.2. Target test loads

To determine the target test loads, partial safety factors have to be incorporated with the design loads. In particular, BS-EN 61400-2:2006 [28] and BS-EN 61400-23:2002 [29] require the inclusion of the product of the following partial safety factors: load γ_f, consequence of failure γ_n and blade to blade manufacturing variations γ_s. It appears that the recommended combined safety factor is similar in various certification standards [39].

As is later revealed, a single-point test method is employed, where a single concentrated point load is applied at l m from the blade root. The target point load F ($F = M_{yB}/l$), associated with the target blade root bending moment M_{yB}, at the normal operation and worst case loads is 1.48 kN and 3.99 kN, respectively.

3.2. Experimental set-up

3.2.1. Test equipment

For the static flap-bending test, a single point test method was employed. The blade root was fixed to a specially designed rigid steel test rig (Fig. 5a) via a simple bolted connection. No inserts or studs are used; rather, the bolts go through holes in the composite sandwich (skin/cap/core/cap/skin). The test rig mimics the real blade root to hub connection, with the same square bolt pattern, plate thickness and plate local geometry. The test rig was attached to two structural poles. The blade was fixed horizontal (flap-wise up) and was loaded by an overhead crane. A composite saddle was specially built to enclose the blade's cross-section at the desired load point. This is presented in Fig. 5b.

The overall loading arrangement is presented in Fig. 6. The external sleeves of the saddle have eyebolts which are used to connect to a 12 kN calibrated load cell. The load cell rests on a spreader beam and is attached to a 5 tonne overhead crane. As the blade deflects, the load direction relative to the blade orientation can change. To ensure that the load is perpendicular to the load application point on the blade, the overhead crane is periodically moved towards the blade root after releasing some load. A spring-loaded marker, attached at the blade tip, provides in situ tip displacement monitoring.

3.2.2. Test regime

To systematically achieve the target point test loads F, a loading sequence was developed (Fig. 7). The test has three stages: (i) loading up to the 100% normal operation load ($F = 1.48$ kN), (ii) loading up to the worst case load ($F = 3.99$ kN, i.e. 270% (=3.99/1.48) of normal operation load), and (iii) loading to failure. To ensure steady loading, small steps of 0.01–0.03 kN are used. Regular load dwells are incorporated to allow the blade to settle.

3.3. Results and discussion

The flax and E-glass blades were subjected to flap-bending tests according to the experimental set-up and loading regime described in Section 3.2. Fig. 8 presents graphs of test load and tip displacement as a function of test duration, for both the blades. It is observed that both the blades survive the normal operation load without any superficial failure and survive the worst case load without any functional/catastrophic failure. As both the blades satisfy the ultimate strength requirements of BS-EN 61400-23:2002 [29], the flax blade can be viewed as a potential replacement to the E-glass blade. The failure load and corresponding tip displacement of the flax blade is 4.14 kN and 2300 mm, respectively. The failure data of the E-glass blade is not disclosed. BS-EN 61400-23:2002 [29] does not formally require measuring the failure load and tip deflection.

Table 5 presents useful information from the graphs in Fig. 8, enabling direct comparison of the performance of the E-glass and flax blades. At normal operation loads, the E-glass blade has a tip deflection of 270 mm while the flax blade has a 40% higher tip deflection of 388 mm. The tip deflections are 8–11% of the blade length. While the flax blade survives the worst case loading like the E-glass blade, the flax blade is significantly more flexible than the E-glass blade. The E-glass and flax blades have a tip displacement of 743 mm and 2025 mm under worst case loading, which is 22% and 60% of the blade length, respectively. To avoid tower strike, BS-EN 61400-23:2002 [29] requires that the tip displacement should be less than the clearance provided between the blade tip and the tower, even at worst case loading. As the traditional practise in designing a turbine is to accommodate the requirements of the blade (i.e. blade-centered design), a turbine can be designed so that a generous clearance is available to accommodate the large tip deflection of the flax blade. A possible design solution is to increase the distance between the rotor centre and tower axis, and use a yaw drive mechanism (or thicker flanges) to balance the increased overturning moment of the rotor. In addition, a modified flax blade design incorporating a spar (with shear webs/caps) will enable major reductions in tip deflection by increasing the flexural rigidity of the blade.

Fig. 5. Image showing the (a) test rig and (b) composite saddle.

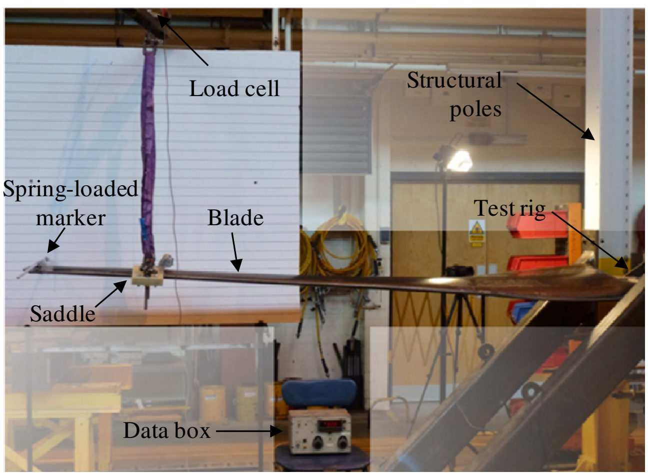

Fig. 6. Blade flap-wise test loading arrangement.

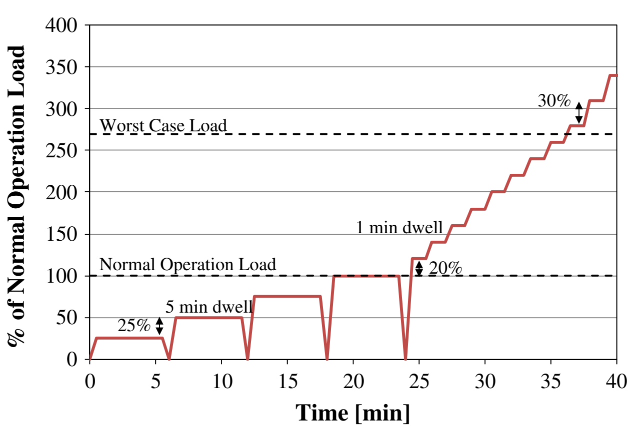

Fig. 7. Blade flap-wise test loading regime. Load values (*y*-axis) are normalised by the normal operation load (of 1.48 kN).

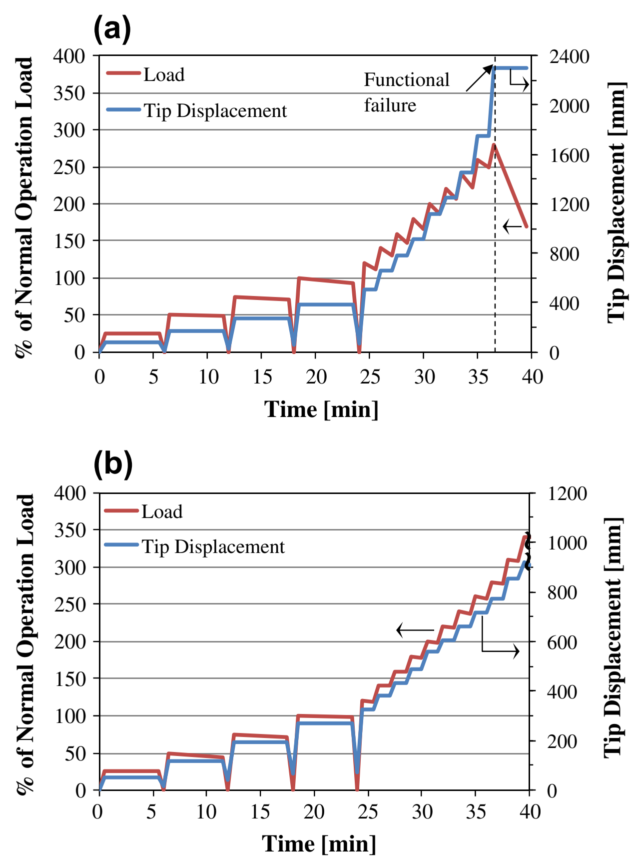

Fig. 8. Test load and tip displacement as a function of time, for the (a) flax and (b) E-glass blades. The point of functional failure has been indicated. Load values (*y*-axis) are normalised by the normal operation load (of 1.48 kN).

The load curves in Fig. 8 show relaxation in loads during dwells. It is observed that load relaxation is much higher in the flax blade than the E-glass blade. In fact, in stage 2, the magnitude of load relaxation averages 0.03 kN for the E-glass blade but 0.18 kN for the flax blade. Interestingly, during periods of load relaxation, the blade tip displacement remains fairly constant. The greater load relaxation in the flax blade implies reducing blade stiffness. This could possibly be due to a poorer fibre/matrix interface resulting in gradual plastic deformation through progressive micro-mechanical damage mechanisms such as fibre/matrix debonding and pull-out. This is common in PFRPs [2,33,40]. In addition, it has been shown that plant fibre composites have a non-linear stress–strain curve, resulting from a very small elastic strain limit of ~0.15%, implying that plastic deformation from micro-damage occurs very early in the load curve [41,42].

3.3.1. Displacement–load curves

Fig. 9 presents tip displacement versus load curves for the flax and E-glass blades. Interestingly, while the tip displacement increases at a constant rate with load (linear growth, $R^2 = 0.996$) for the E-glass blade, the tip displacement increases at an increasing rate with load (quadratic growth, $R^2 = 0.989$) for the flax blade. This is in agreement with the load–displacement curve of the different materials. E-glass composites have a linear load–displacement

Table 5
Loads and corresponding tip displacements of the E-glass and flax blades, at the end of test stages 1, 2 and 3.

	Flax blade				E-glass blade			
	Load		Tip displacement		Load		Tip displacement	
Stage of test loading	kN	% Of NO[a] load	mm	% Of blade length	kN	% of NO[a] load	mm	% Of blade length
Normal operation	1.48	100	388	11	1.48	100	270	8
Worst case	3.99	270	2030	60	3.99	270	743	22
Failure	4.14	280	2300	68	N/A[b]	N/A[b]	N/A[b]	N/A[b]

[a] NO load is 'normal operation' load.
[b] Non-disclosable data.

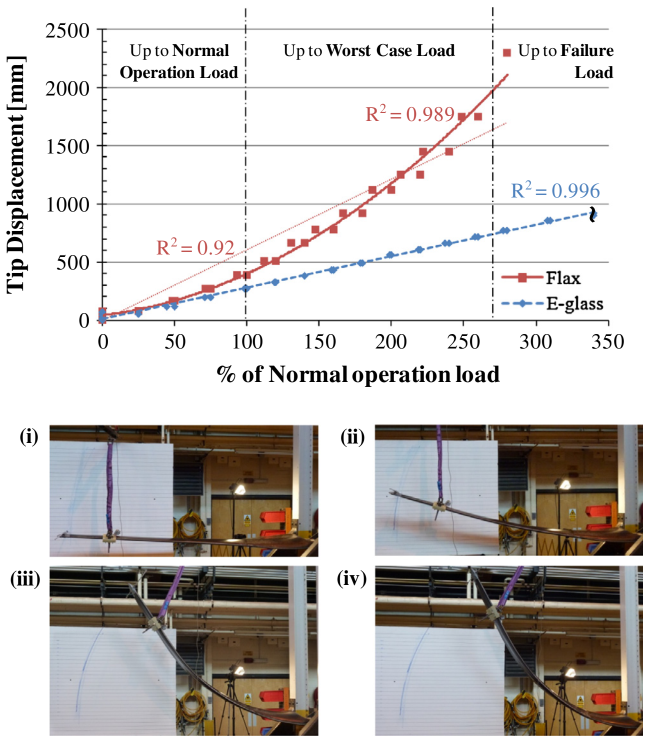

Fig. 9. Tip displacement versus load curves for the flax and E-glass blades. Images of the flax blade under (i) no load, (ii) normal operation load, (iii) worst case load, and (iv) failure load, are also presented. Load values (x-axis) are normalised by the normal operation load (of 1.48 kN).

curve, while plant fibre composites have a non-linear load–displacement curve [41–44]. In particular, plant fibre composites exhibit softening (i.e. decreasing stiffness with increasing strain/load) [41,43]. Shah et al. [41] have shown that the stiffness of flax/polyester composites reduces by up to 30% in the 0–0.25% strain range, while the stiffness of E-glass composites is fairly constant. This highlights the differing stress–strain accumulation and damage-growth mechanisms in E-glass reinforced composites and plant fibre reinforced composites, particularly due to the differing fibre structure and morphology and fibre/matrix interactions.

Fig. 9 clearly demonstrates the significantly higher deflection of the flax blade in comparison to the E-glass blade. Fig. 9 also presents images of the flax blade under (i) no load, (ii) normal operation load, (iii) worst case load, and (iv) failure load.

3.3.2. Flexural rigidity of blades in the flap-wise direction

Two strategies are available to estimate the flexural rigidity (EI) of a blade. The first technique involves assuming that the blade can be considered as a uniform cross-section cantilever beam subjected to a single concentrated load at l m from the blade root. Assuming small deflections and applying appropriate boundary conditions at the ends of the cantilever beam, the mean flexural stiffness EI_{mean} of a blade can be then estimated by applying simple static analysis using Macaulay's method (Eq. (1)). In Eq. (1), y_{tip}/F is the slope of the tip displacement to load curve, z_{tip} (=3.50 m) is the length of the blade and l is the distance between the point of load application along the blade from the blade root. Importantly, this simple analysis conveniently shows that the blade flexural stiffness is inversely proportional to the slope of the tip displacement to load curve.

$$EI_{mean} = \frac{K}{y_{tip}/F}, \quad K = \frac{[z_{tip} - l]^3}{6} - \frac{z_{tip}^3}{6} + \frac{l z_{tip}^2}{2} \tag{1}$$

Using the slope (y_{tip}/F) of the linear tip displacement–load curve for the E-glass blade (181.6 mm/kN) and the flax blade (408.8 mm/kN) from Fig. 9 and substituting the relevant constants in Eq. (1), the mean flexural stiffness EI_{mean} of the E-glass and flax blades is found to be 53.1 kN m^2 and 23.6 kN m^2, respectively. That is, the flax blade is 2.25 times more flexible than the E-glass blade. As the displacement–load curve for flax is non-linear and follows a quadratic equation better, a better approximation of EI_{mean} can be obtained if the differential of the best-fit quadratic equation is taken as y_{tip}/F. The mean flexural stiffness EI_{mean} of the flax blade is then a function of load, and is found to reduce with increasing load. For instance, EI_{mean} at loads of 0 kN, 1.48 kN (normal operation load) and 3.99 kN (worst case load) is 96.9 kN m^2, 25.1 kN m^2 and 11.1 kN m^2, respectively.

An alternate, and more rigorous, method to estimate the flexural rigidity of the blade involves measuring the vertical deflection (using the video footage) of a blade subjected to normal operation loads at various points along the blade. 18 points along the leading and trailing edges are used for deflection measurement. From the vertical deflections, the bending angle $\theta = dy/dz$, and bending rate per unit length $d\theta/dz$ can be calculated using finite difference methods. The flexural rigidity at different points along the blade can then be determined by using Eq. (2) [45]. The results for the E-glass and flax blades are presented in Fig. 10. The curves observed have a similar profile to those found in literature for larger GFRP wind turbine blades [45].

$$EI = \frac{M}{d\theta/dz}, \quad d\theta/dz = d^2y/dz^2 \tag{2}$$

Fig. 10a shows the applied bending moment along the blade length z due to the point load at l m from the blade root. Note that the applied bending moment is null beyond the load application point. In addition, the bending moment at the blade root is the required target blade root bending moment M_{yB} of 4.15 kN m. The resulting vertical deflection along the blade length of the E-glass and flax blades can be observed in Fig. 10b. The deflection profile for both blades is observed to follow a quadratic equation ($R^2 > 0.995$). It is clearly observed that the flax blade deflects more than the E-glass blade. The calculated bending angle along the blade lengths for the two blades is presented in Fig. 10c. The bending angle is observed to increase fairly linearly with blade

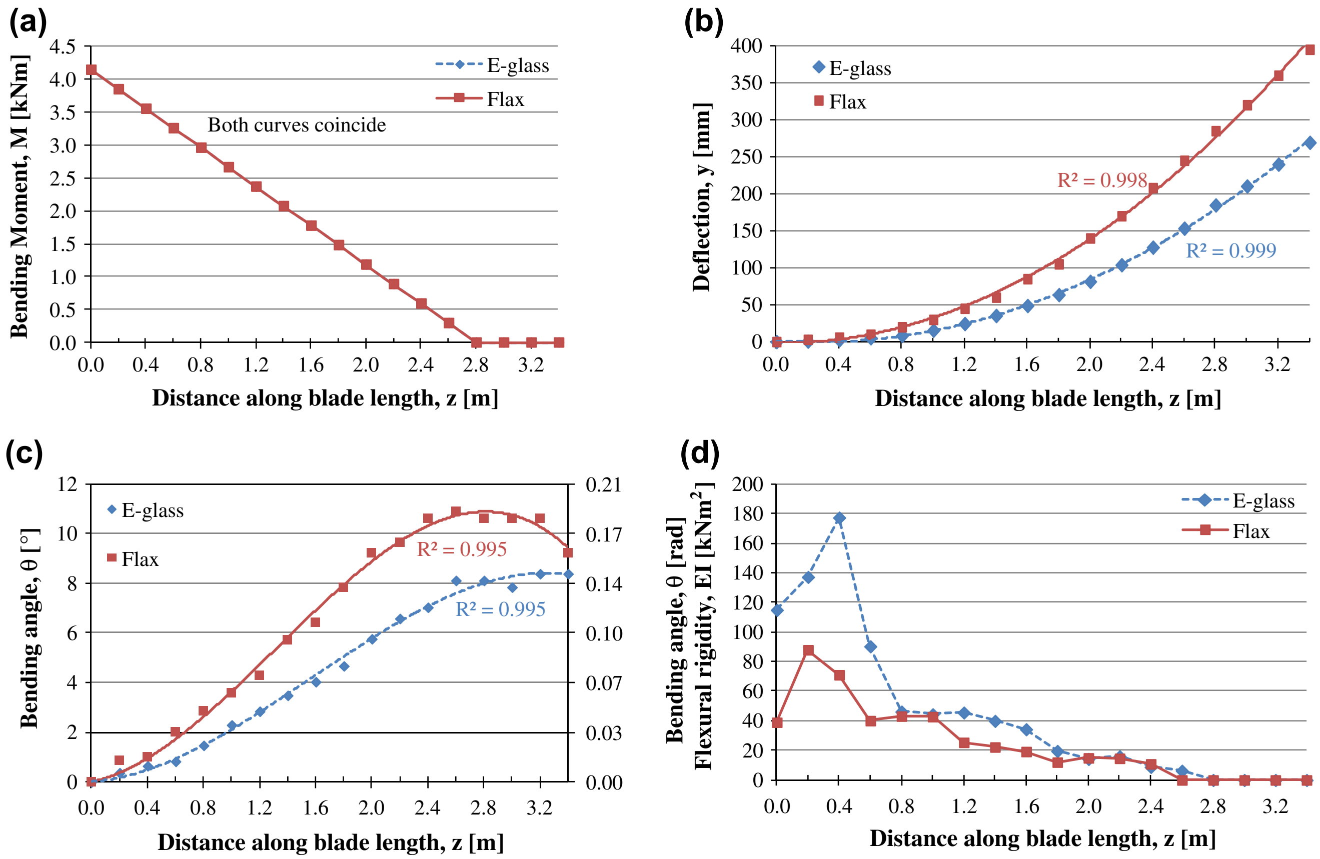

Fig. 10. Graphs showing the variation in (a) applied bending moment, (b) vertical deflection, (c) bending angle and (d) flexural rigidity, along the blade length, for the flax and E-glass blades, when subjected to normal operating test loads (of 1.48 kN).

length up to the load application point, after which it becomes constant. This is because beyond this load application point there is no bending moment (Fig. 10a).

Fig. 10d illustrates the variation in estimated flexural rigidity *EI* along the blade length for both the blades. The higher flexural rigidity at close to the blade root is due to the higher bending moment of area and presence of more layers of unidirectional reinforcement. Sudden dips in the flexural rigidity along the blade length are possibly due to step-changes in the stacking sequence of the blade.

It is observed that the E-glass blade exhibits a higher flexural rigidity at almost all points along the blade length. In particular, the flexural rigidity of the E-glass blade is 2–3 times more than the flax blade, along the first meter of the blade. Using the trapezium rule, an indicative value of the mean flexural stiffness for the blades can be determined. EI_{mean} is found to be 43.4 kN m^2 for the E-glass blade and 24.6 kN m^2 for the flax blade. These values are fairly similar to those calculated previously through the simple static analysis method.

In comparing the mechanical properties of flax and E-glass composites in Table 2, it was found that the stiffness of flax composites is 83% that of E-glass composites (at $v_f = 100\%$). On the other hand, the mean flexural rigidity of the flax blade is 57% that of an identical construction E-glass blade. Hence, it is interesting to see that while flax fibres and their composites are recognized for their stiffness [2,33,46], a flax blade (i.e. component/structure) cannot compete against an E-glass blade in terms of stiffness. Furthermore, despite the well-documented poor strength properties of flax composites (in comparison to GFRPs; Table 2), the flax blade, like the E-glass blade, is able to withstand the worst case loads. This shows that more studies are required to understand the behaviour of PFRPs when employed in specific applications/structures, rather than limiting materials analysis to data extracted from coupon testing.

3.3.3. Failure modes of blades

The E-glass and flax blades failed under different modes, as is depicted by Figs. 11 and 12. The E-glass blade failed due to crack formation at the root-hub junction. Upon further loading, the crack grew across the blade cross-section causing extensive delamination. Fig. 11 shows how the composite laminates have peeled from the core. The crack eventually grows to such an extent that the trailing edge, along the maximum chord length, split open.

Fig. 11. The E-glass blade, failing at the blade root, exhibited extensive delamination.

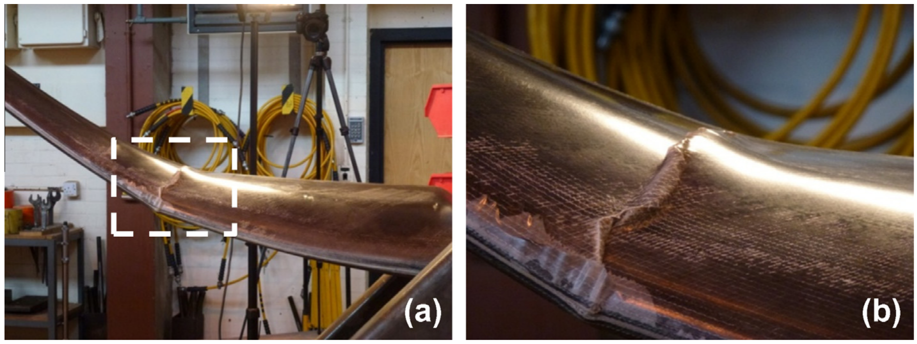

Fig. 12. Images of the fractured flax blade showing (a) the region of failure, and (b) wrinkle formation due to buckling.

On the other hand, the flax blade failed ~1 m along the blade length from the blade root (Fig. 12a) which corresponds to a step-change in the stacking sequence. This point of step-change is a possible stress-raiser. Hence, as the load exceeded 4 kN and the tip deflection approached 70% of the blade length, the stress concentration increased substantially. Initially, matrix cracking/peeling was observed (Fig. 12b) – a sign of resin richness. Then, the top surface, experiencing compressive loads, buckled. The wrinkles and delamination resulting from the compressive failure of the composite laminate can be seen in Fig. 12b. Further loading led to complete buckling, delamination and eventually collapse of the blade.

4. Conclusions

Through this novel comparative case study, the manufacture and mechanical testing of 3.5 m composite rotor blades (suitable for an 11 kW turbine) built from flax/polyester and E-glass/polyester has been investigated. The lower density of plant fibres expectedly enables component weight savings; it is found that the flax/polyester blade is 10% lighter than the E-glass/polyester blade (fibre mass saving of 45%). Static flap-wise testing of the blades, in accordance to certification standards, confirmed that like the E-glass/polyester blade, the flax/polyester blade satisfies the design and structural integrity requirements for an 11 kW turbine, under normal operation and worst case loading. While the displacement–load curve is linear for the E-glass blade, it is non-linear for the flax blade, highlighting the varying stress–strain accumulation mechanisms in natural materials. The mean flexural rigidity of the flax and E-glass blades are 24.6 kN m^2 and 43.4 kN m^2. Design solutions have been offered to overcome the larger tip deflection of the flax blade. For instance, to improve the rigidity of the flax blade, it is suggested that an improved blade design, which incorporates a spar (with shear webs/caps), is trialled. The flax and E-glass blades are found to fail in a different manner. The failure load and corresponding tip displacement of the flax blade is 4.14 kN and 2300 mm, respectively.

In conclusion, it is proposed that flax is a suitable structural replacement to E-glass for similar composite small wind turbine blade applications. In view of the findings of this research, it is suggested that (i) the development of low-cost aligned plant fibre semi-products is a limiting factor to the industrial uptake of PFRPs in structural applications, and (ii) more ambitious studies are required to understand the behaviour of PFRPs when employed in specific applications/structures, rather than limiting materials analysis to data extracted from coupon testing.

Acknowledgements

This project is supported by the Nottingham Innovative Manufacturing Research Centre (EPSRC, Project title ‘*Sustainable manufacture of wind turbine blades using natural fibre composites and optimal design tools*’).

References

[1] Shah D, Schubel PJ, Licence P, Clifford MJ. Hydroxyethylcellulose surface treatment of natural fibres: the new ‘twist’ in yarn preparation and optimization for composites applicability. J Mater Sci 2012;47:2700–11.
[2] Wambua P, Ivens J, Verpoest I. Natural fibres: can they replace glass in fibre reinforced plastics? Compos Sci Technol 2003;63:1259–64.
[3] Faruk O, Bledzki AK, Fink HP, Sain M. Biocomposites reinforced with natural fibres: 2000–2010. Prog Polym Sci 2012;37(11):1552–96.
[4] Reux F. Worldwide composites market: main trends of the composites industry. In: 5th Innovative composites summit – JEC ASIA 2012. Singapore; 2012.
[5] Shahzad A. Hemp fiber and its composites – a review. J Compos Mater 2012;46(8):973–86.
[6] Carus M. Bio-composites: technologies, applications and markets. In: 4th International conference on sustainable materials, polymers and composites. Birmingham, UK; 6–7 July 2011.
[7] Pickering K. (Ed.), Properties and performance of natural-fibre composites. Boca Raton: CRC Press LLC; 2008.
[8] Joshi S, Drzal LT, Mohanty AK, Arora S. Are natural fiber composites environmentally superior to glass fiber reinforced composites? Compos A Appl Sci Manuf 2004;35:371–6.
[9] Carus M, GC. Natural fibre reinforced plastics – material with future. Huerth: nova-Institut GmbH; 2008
[10] Bos H. PhD thesis: the potential of flax fibres as reinforcement for composite materials. Technische Universiteit Eindhoven: Eindhoven, Netherlands; 2004
[11] Bledzki A, Faruk O, Sperber VE. Cars from bio-fibres. Macromol Mater Eng 2006;291:449–57.
[12] Opportunities in natural fiber composites. Las Colinas, USA: Lucintel; 2011.
[13] Carus M, Gahle C. Natural fibre reinforced plastics – material with future. Huerth: nova-Institut GmbH; 2008.
[14] Ticoalu A, Aravinthan T, Cardona F. A review of current development in natural fiber composites for structural and infrastructure applications. In: Southern region engineering conference. Australia: Toowoomba; 11–12 November 2010.
[15] van Rijswijk K, Brouwer WD, Beukers A. Application of natural fibre composites in the development of rural societies. Delft, Netherlands: Delft University of Technology; 2001.
[16] Fowler P, Hughes JM, Elias RM. Biocomposites: technology, environmental credentials and market forces. J Sci Food Agric 2006;86:1781–9.
[17] Dittenber D, Gangarao HVS. Critical review of recent publications on use of natural composites in infrastructure. Compos A Appl Sci Manuf 2012;43:1419–29.
[18] Sharma R, Raghupathy VP, Rao SS, Shubhanga P. Review of recent trends and developments in biocomposites. In: International conference on recent developments in structural engineering. Manipal, India; 2007.
[19] Riedel U, Nickel J. Natural fibre-reinforced biopolymers as construction materials – new discoveries. Die Angewandte Makromolekulare Chemie 1999;272:34–40.
[20] Kalia S, Dufresne A, Cherian BM, Kaith BS, Avérous L, Njuguna J, et al. Cellulose-based bio- and nanocomposites: a review. Int J Polym Sci 2011. http://dx.doi.org/10.1155/2011/837875.
[21] Riedel U. 10.18 – Biocomposites: long natural fiber-reinforced biopolymers. Polymer science: a comprehensive reference. Polym Sust Environ Green Energy 2012;10:295–315.
[22] Yu H, Kim SS, Hwang IU, Lee DG. Application of natural fiber reinforced composites to trenchless rehabilitation of underground pipes. Compos Struct 2008;86:285–90.
[23] Bledzki A, Gassan J. Composites reinforced with cellulose based fibres. Prog Polym Sci 1999;24:221–74.

[24] Bio-composites update: bio-based resins begin to grow. 4/1/2008 <http://www.compositesworld.com/articles/bio-composites-update-bio-based-resins-begin-to-grow.aspx> [cited 12.12.09].
[25] Auto body made of plastics resists denting under hard blows, in popular mechanics magazine, vol. 76 (6); 1941. p. 12.
[26] A fighter fuselage in synthetic material. Duxford, Cambridge: Aero Research Limited; October 1945.
[27] Small wind systems – UK market report. London: Renewable UK (BWEA); 2011.
[28] BS EN 61400-2:2006. In wind turbines – Part 2: design requirements for small wind turbines. London: British Standards Institution; 2006.
[29] BS-EN 61400-23:2002. In wind turbine generator systems – Part 23: full-scale structural testing of rotor blades. London: British Standards Institution; 2002.
[30] Shah D, Schubel PJ, Clifford MJ, Licence P. Fatigue characterisation of plant fibre composites for small-scale wind turbine blade applications. In: 5th Innovative composites summit – JEC Asia 2012. Singapore; 2012.
[31] Shah, D., Schubel PJ, Clifford MJ, Licence P, Fatigue characterisation of plant fibre composites for rotor blade applications, in JEC composites magazine, No. 73: special JEC Asia. Paris: JEC Composites; June 2012. p. 51–4.
[32] Mwaikambo L, Ansell MP. Chemical modification of Hemp, Sisal, Jute and Kapok fibers by alkalization. J Appl Polym Sci 2002;84:2222–34.
[33] Shah D, Schubel PJ, Clifford MJ, Licence P, Mechanical characterization of vacuum infused thermoset matrix composites reinforced with aligned hydroxyethylcellulose sized plant bast fibre yarns. In: 4th International conference on sustainable materials, polymers and composites. Birmingham, UK; 6–7 July 2011.
[34] Shah D, Schubel PJ, Clifford MJ, Licence P. Fatigue life evaluation of aligned plant fibre composites through *S–N* curves and constant-life diagrams. Compos Sci Technol 2013;74:139–49.
[35] Shah DU, Schubel PJ, Clifford MJ. Modelling the effect of yarn twist on the tensile strength of unidirectional plant fibre yarn composites. J Compos Mater 2013;47(4):425–36.
[36] Lewin M. Handbook of fiber chemistry. 3rd ed. Boca Raton: CRC Press LLC; 2007.
[37] Madsen B. PhD thesis: properties of plant fibre yarn polymer composites – an experimental study. In: Department of civil engineering. Technical University of Denmark; 2004
[38] Shah D, Schubel PJ. Full-scale structural testing of a rotor blade. Nottingham: The University of Nottingham; 2012.
[39] Wacker G. Requirements for the certification of rotor blades. In: SAMPE 2003 – advancing materials in the global economy – applications, emerging markets and evolving technologies. California: Long Beach, May 11–15; 2003.
[40] Kalia S, Kaith BS, Kaur I. Pretreatments of natural fibers and their application as reinforcing material in polymer composites-a review. Polym Eng Sci 2009:1253–72.
[41] Shah D, Schubel PJ, Clifford MJ, Licence P. The tensile behavior of off-axis loaded plant fiber composites: an insight on the non-linear stress-strain response. Polym Compos 2012;33(9):1494–504.
[42] Hughes M, Carpenter J, Hill C. Deformation and fracture behaviour of flax fibre reinforced thermosetting polymer matrix composites. J Mater Sci 2007;42:2499–511.
[43] Baets, J, Plastria D, Ivens J, Verpoest I, Determination of the optimal flax fibre preparation for use in UD-epoxy composites. In: 4th International conference on sustainable materials, polymers and composites. Birmingham, UK; 6–7 July 2011.
[44] Baley C. Analysis of the flax fibres tensile behaviour and analysis of the tensile stiffness increase. Compos A Appl Sci Manuf 2002;33:939–48.
[45] McKittrick L, Cairns DS, Mandell J, Combs DC, Rabern DA, van Luchene RD, SAND2001-1441: analysis of a composite blade design for the AOC 15/50 wind turbine using a finite element model. Livermore, California: Sandia National Laboratories; 2001.
[46] Goutianos S, Peijs T, Nystrom B, Skrifvars M. Development of flax fibre based textile reinforcements for composite applications. Appl Compos Mater 2006;13(4):199–215.